Programmable Design of Seed Coating Function to Induce Water Stress Tolerance in Semi-Arid Regions

Augustine T. Zvinavashe, Julie Laurent, Salma Mouhib, Hui Sun, Henri Manu Effa Foud, Doyoon Kim, Manal Mhada, Lamfeddal Kouisni, Benedetto Marelli

Affiliations

Department of Civil and Environmental Engineering, Massachusetts Institute of Technology, Cambridge, MA, United States

Augustine T. Zvinavashe, Julie Laurent, Hui Sun, Henri Manu Effa Foud, Doyoon Kim, Benedetto Marelli

AgroBioSciences Research Division, Mohammed VI Polytechnic University, Ben-Guerir, Morocco

Salma Mouhib, Manal Mhada, Lamfeddal Kouisni

A.T.Z. and J.L contributed equally

Benedetto Marelli – bmarelli@mit.edu

Keywords: silk fibroin, mucilage, biofertilizers, rhizobacteria, arid, food security

Abstract

Changes in climate patterns and soil depletion are major challenges that agriculture needs to address to build a sustainable food infrastructure that can feed the growing human population. In semi-arid regions, water is the determining factor for crop production and water stress during seed germination and early seedling growth is the highest cause of crop loss, with dramatic impact on food security for 1 billion people that are threatened by desertification. In nature, some seeds (e.g. chia, basil) produce a mucilage-based hydrogel that creates a germination-promoting microenvironment by retaining water, regulating nutrients entry, and facilitating interactions with beneficial microorganisms. Inspired by this strategy, a two-layered biopolymer-based seed coating has been developed to increase germination and water stress tolerance in semi-arid, sandy soils. Seeds are coated with a silk/trehalose inner layer containing *rhizobacteria* and with a pectin/carboxymethylcellulose (CMC) outer layer that upon sowing reswells and acts as a water jacket. Using *Phaseolus vulgaris* (common bean) cultured under water stress conditions in an experimental farm in Ben Guerir, Morocco, it is demonstrated that the proposed seed coating effectively delivers *rhizobacteria* to form roots nodules, results in plants with better health, and mitigates water stress in drought-prone marginal lands.

Main

The projected growth of the human population together with changes in climate patterns will significantly challenge the food infrastructure[1] and require the development of new technologies[2–8] to enable sustainable food production while minimizing the use of scarce resources (e.g. water, fertile land), reducing the application of energy intensive inputs (e.g. synthesis of nitrogen-based fertilizers consumes 1-2% of the global energy production) and mitigating environmental impact.[9,10] In semi-arid regions, which constitute circa 15% of the world's land, water is the determining factor for crop production[11] and water stress during seed germination and early seedling growth is the highest cause of crop loss,[12] with dramatic impact on food security for 1 billion people that are threatened by desertification and already live in conditions of malnutrition.[13]

For semi-arid soils, water-holding compounds like hydrophilic and superabsorbent polymers can be applied to seeds, mixed into the soil or deposited on roots before planting to increase water retention and usage efficiency.[14–16] However, the application of these polymers is labor and energy intensive and often results in the release of synthetic plastics in the soil.[17] As a complementary approach, plant-growth promoting rhizobacteria (PGPRs) can be used to enhance plant health in conditions of water scarcity.[18–21] PGPRs are biofertilizers that interact with plant roots to increase availability of nutrients and phytohormones and enhance plant response to heat, saline soil and drought.[22–25] Some PGPRs, like rhizobia, can infect legume roots to form symbiotic nodules that fix nitrogen, limiting the use of fertilizers and enhancing plant health in semi-arid regions.[26–28] Nonetheless, the use of PGPRs is limited by their low resistance to desiccation stress[29,30] and competition upon resuscitation with a diversity of microorganisms present in the soil environment (i.e. spermosphere)[31]. Together, these limitations make difficult the integration of rhizobia in simple delivery systems – as seed coating technologies – that do not require the use of skills, agricultural practices and resources often not available in semi-arid regions of the world.[32]

In nature, polysaccharides present in the seed coat of myxospermous species occupying arid environments (e.g. *Salvia hispanica*, *Ocimum basilicum* and *Plantago ovata*) swells and extrudes, upon sowing, a halo of mucilage that completely envelops the seed.[33–35] The extruded mucilage generates a growth-promoting spermosphere that retains water, regulate nutrients entry, and facilitates interactions with PGPRs.[33] Seed mucilage is of increasing interest for the pharmaceutical, biomedical and food industry and it is usually a composite of pectic, non-cellulosic, and cellulosic polysaccharides.[36] In this study, we have been inspired by the multifunctional coat of myxospermous seed to develop a seed coating technology with programmable function that creates a spermosphere that positively affects the seed niche and promotes water stress-resistance in semi-arid soils.

Results

Seed coating

The coating consists of a two-layered structure (Fig. 1). An SEM image of the dry two layered coating deposited on the surface of a *Phaseolus vulgaris* seed is depicted in Fig. 1a. The inner layer (Layer 1) is made of a 1:3 by weight mixture of silk fibroin and trehalose that contains *Rhizobium tropici* CIAT 899 – referred to as *R. tropici* CIAT 899 onwards. Silk fibroin is a 395kDa structural protein that is extracted from the *Bombyx mori* silk cocoon with a yield of 70-75% and is the main component of the silk textile fibers.[37,38] Through a water-based process applicable also to silk waste – cocoons unsuitable for reeling, yarn waste and garneted stock – silk fibroin can be regenerated in a water suspension and then easily applied to form coatings through dip-coating and spray-coating techniques.[39] The physical, mechanical, biological and biodegradation properties of silk fibroin can be modulated by controlling the protein secondary and tertiary structures (random coil, alpha helix and beta-sheet) at the point of material assembly or with post-processing techniques (silk fibroin polymorphism).[40–44] Silk fibroin is also known to preserve biological entities and

101 biomolecules encapsulated in silk-based materials by providing a barrier to oxygen stress and
102 minimize contact with water.[45] Trehalose is a disaccharide ubiquitously used by natural
103 organisms to impart osmoprotection and that can act as carbon source for rhizobium.[46–48] The
104 mixture of silk fibroin and trehalose enables Layer 1 adhesion to the seed coat, preservation of
105 *R. tropici* CIAT 899 by mitigating oxidative and osmotic stresses, and release of the
106 biofertilizer upon sowing,[45,48,49] Given Layer 1 coating thickness (t), an ellipsoidal seed shape
107 (a, b, c), the known concentration of *R. tropici* CIAT 899 (C_a) and assuming a homogeneous
108 dispersion of *R. tropici* CIAT 899 and the formation of a homogeneous coating, it is possible
109 to estimate the number of *R. tropici* CIAT 899 in the inoculum (N) by multiplying C_a with the
110 volume (V) as shown in equation (1).

111 $$N = C_a \times V = C_a \times \left(\frac{4}{3}\pi ABC - \frac{4}{3}\pi abc\right) \qquad (1),$$

112 where A=a+t, B=b+t, and C= c+t. Using a = 0.25 cm, b = 0.25 cm, c = 0.5 cm, t = 0.000 5cm,
113 and $C_a = 10^{10}/cm^3$, then N = $6.56*10^6$ *R. tropici* CIAT 899 were encapsulated per seed. The
114 external layer (Layer 2) is a mucilage-like mixture of pectin-carboxymethyl cellulose (P:C
115 1:1) that contains nutrients and upon sowing forms a hydrogel that acts as a water jacket and
116 provides a suitable environment for rhizobia resuscitation and growth (Fig. 1a-b). Layer 2 was
117 designed as food gel[50] and contains Ca^{2+} ions that act as crosslinker for pectins' galacturonic
118 acid residues, providing stability to the gel and yielding a gel content of circa 65% (Fig. 1c).
119 CMC molecules present in Layer 2 fill the gaps in the pectin network and confer water
120 superabsorption properties and enhance water retention. In Supplementary Fig.1, we report
121 the investigation of P:C hydrogels volume variation in 154 mM NaCl solution due to water
122 absorption and gel content (GC) as a function of relative pectin and carboxymethyl cellulose
123 (CMC) content and of increasing Ca^{2+} concentrations. Volume variation upon re-hydration
124 and GC of pectin, CMC and their mixtures indicated that P:C 1:1 provides the best
125 performance as a trade-off between volume variation (indication of water uptake) and GC

126 properties (indication of gel stability over time). The effects of biologically-relevant low,
127 medium and high Ca^{2+} concentrations in P:C gels (5 mM or LCC, 10 mM or MCC and 15 mM
128 or HCC) were then investigated, given the strong beneficial effect of the dication on rhizobia
129 symbiosis with leguminous plants[51]. P:C 1:1 volume increased in the first three hours upon
130 rehydration, decreased at the 6 h time point, recovered and plateaued at 12 h (Fig. 1e). The
131 decrease in volume at 6 h was similar for all the materials considered and could be explained
132 with the wash-off of non-crosslinked CMC molecules. Previously reported maximum
133 swelling of pectin hydrogels crosslinked with glutaraldehyde matched the results obtained in
134 this study,[52] though the use of toxic crosslinkers should be avoided for agricultural
135 applications.[53,54] Further, studies of biodegradable hydrogels used to modify soil water
136 holding capacity have reported water absorption in the same order of Layer 2.[55] Water
137 retention is another important parameter to consider in semi-arid soils as the hydrogels can
138 stabilize the humidity around seeds for extended periods of time, acting as a water buffer in-
139 between watering periods[56]. The measurement of volume variation during air-drying indicated
140 that all the P:C gels considered had similar water loss trends, but HCC and MCC gels could
141 retain water longer than LCC, given the higher initial volumes (Fig. 1f). The use of different
142 pectin to CMC ratio in P:C and lower concentrations of Ca^{2+} ions may further be used to
143 regulate water retention (Supplementary Fig. 2). Water absorption studies for gels were also
144 conducted in soil, to simulate how Layer 2 would swell upon sowing. Volume variations of
145 gels were measured after 24h in three soil water content (SWC) conditions (Fig. 1g). Gels'
146 volume significantly increased with SWC ($p<0.05$), but Ca^{2+} ions did not have statistically
147 significant effect on the swelling for the concentrations considered ($p>0.05$). Interestingly, an
148 order of magnitude was lost in P:C water uptake, when compared to swelling in saline
149 solution, probably due to the lower water potential of soil and the compressive forces that soil
150 applies on the gel and that limit swelling. However, even in semi-arid soils (SWC=10%),
151 volume variation around 250% indicated the capability of the coating to extract water from

152 the environment and make it available to the rhizobacteria and the seed. A pressure of circa
153 412 Pa is applied on the surface of a *P. vulgaris* seed (1.4x0.8x0.7 cm) sowed 3 cm below the
154 surface of a semi-arid soil ($\rho_{avg} \cong 1.4$ g/cm^3). Additionally, soil has a compression modulus of
155 circa 4-7 MPa[57], indicating that the hydrogels may have complex interactions with the
156 surrounding soil while reswelling occurs as a combination of soil deformation and expansion
157 in air pockets present in the soil.[58]
158
159 Mechanical Properties and Gel Microstructure
160 Rheological measurements help to choose the required settings for material application
161 onto seed surface. Rheological investigation of LCC, MCC and HCC solutions (i.e. before
162 gelling is triggered) showed a shear thinning behavior (Supplementary Fig. 3) and the stability
163 of the solutions' storage and loss modulus (G' and G'', respectively) (Fig. 2a) over time upon
164 addition of Ca^{2+} ions into the P:C suspension. Exposure of P:C suspension to NaOH, causes a
165 rapid increase in pH that results in immediate gelation of LCC, MCC and HCC. The rapid
166 gelation hinders the application of the Winter-Chambon rule to calculate gelation time.
167 Nonetheless, the evolution of G' and G" post gelling was monitored over time (Fig. 2b) and
168 showed an increase of G" that was positively correlated with Ca^{2+} concentration. To further
169 evaluate the suitability of P:C gels to work as seed coating, we measured the mechanical
170 properties of P:C 1:1 hydrogels through unconfined compression tests (Fig. 2c). MCC
171 hydrogels displayed both the highest compressive strength (5.43 ± 0.31 kPa) (Fig. 2d) and
172 Young's modulus (33.86 ± 4.60 kPa) (Fig. 2e). Nanoindentation tests were also conducted on
173 dry P:C to determine their capability to sustain transportation and storage periods without
174 being damaged. The measured Young's modulus (~ 15-20 GPa, Fig. 2e) and hardness (~1-1.5
175 GPa, Fig. 2f) were of the same order of currently available seed coatings.[59] Cross-sectional
176 cryo-SEM was used to evaluate the microsctructure of the hydrogels. Micrographs showed an
177 interconnected microstructure with an assumed pore size of ~ 5 μm (Supplementary Fig. S4).

178 However, the pore shape and dimension may have been affected by the formation of ice
179 crystals during the sample preparation, which is known to artificially increase the pore size,
180 particularly in hydrogels with a weak structural integrity such as LCC.[60]
181
182 Support of rhizobacteria growth
183 To investigate the effectiveness of P:C hydrogels as niche to support *R. tropici* CIAT 899
184 resuscitation and growth, we designed two experimental set-ups. In the first study, *R. tropici*
185 CIAT 899 were released from dissolving silk films into swelling P:C 1:1, as shown in Fig. 3a.
186 In particular, we used *R. tropici* CIAT 899 harboring a green fluorescent protein reporter (*R.*
187 *tropici* CIAT 899-GFP) to use the fluorescent intensity signal over time as an indication of
188 bacterial colonization and growth. After verifying that *R. tropici* CIAT 899-GFP could use
189 seed mucilage as carbon source (using simulated basil mucilage as an example,
190 Supplementary Fig. 5), we investigated the migration of *R. tropici* CIAT 899-GFP from silk
191 film into P:C 1:1 formed at increasing concentrations of Ca^{2+} (Fig. 3a) and containing
192 nutrients found in seed mucilage (*i.e.* 20.9 mM (D-(+)-xylose, 6.28 mM L-(+)-arabinose, 6.28
193 mM DL-arabinose, L-8.94 mM rhamnose with a ratio of 30:9:9:14)).[61]
194 The release of *R. tropici* CIAT 899-GFP from silk films and the subsequent P:C
195 colonization was investigated using fluorescent microscopy (Fig. 3b)[62]. Silk films were
196 dissolving gradually over time while green spots, corresponding to *R. tropici* CIAT 899-GFP
197 microcolonies, were growing in size and numbers within the depth of the hydrogels. *R.*
198 *tropici* CIAT 899-GFP microcolonies were more concentrated at the surface of the LCC and
199 HCC gels at day 7, while *R. tropici* CIAT 899 -GFP colonization was more homogenously
200 distributed in MCC samples. Interestingly, a size gradient could be observed in microcolonies
201 present in MCC hydrogels, with larger colonies visible closer to the source of *R. tropici* CIAT
202 899-GFP. To further investigate hydrogel colonization from the environment, we designed a
203 second study where dry P:C 1:1 were immersed in a solution containing *R. tropici* CIAT 899-

204 GFP. GFP intensity in the hydrogels increased over time and plateaued at 32h (Fig. 3c). GFP
205 intensity was inversely proportional to the crosslinker content, i.e. the lower the content of
206 Ca^{2+} ions the higher the GFP intensity. To determine the interplay between Layer 2 swelling
207 and bacteria colonization, we immersed dry P:C 1:1 in a 154 mM solution containing *R.*
208 *tropici* CIAT 899-GFP (OD_{600} ~0.1). Histological sections at 6h and 54h post re-hydration
209 showed the presence of gram-negative *R. tropici* CIAT 899-GFP within the gels (Fig. 3d and
210 Supplementary Fig. 6), suggesting that Layer 2 swelling may be able to recruit endogenous
211 microorganism present in the soil and further attract them post-swelling due to the presence of
212 nutrients in the hydrogel. To further support this assumption, diffusion of saccharides in the
213 hydrogel was studied using fluorescein as a working model. Calculated diffusion coefficients
214 were ~10^{-5} cm^2/s and not influenced by the amount of crosslinks present in the hydrogels (i.e.
215 Ca^{2+} concentration during material fabrication) (Fig. 3e and 3f).[63] This result suggests that the
216 rate of diffusion of nutrients was not the determining factor of *R. tropici* CIAT 899-GFP
217 growth, but other features such as different pore sizes and geometries may have caused an
218 increased colonization in MCC gels.[64,65]
219
220 Coating biodegradation
221 The biodegradation of the seed coating was evaluated by exposing MCC hydrogels to soil.
222 Biopolymers degradation in the absence of light is mostly catalyzed by microbial activity
223 through enzymatic degradation that accelerate proteolytic and carbohydrolytic processes.
224 Important parameters such as type of indigenous microorganisms, temperature, soil type,
225 composition, pH, salinity, water and carbon contents play prominent roles in determine how
226 quickly biopolymers may be degraded. Fig. 4a depicts the mass loss of MCC hydrogels over
227 time when investigated at 16°C in a soil containing microorganisms. At day 14 and 28, almost
228 50% and 70% of the dry weight of the gel was lost. When exposed to soil containing sodium
229 azide – a bacteriostat – the mass loss rate of MCC decreased for the first 14 days, when

230 compared to untreated soil, indicating the critical role of microorganism in biopolymer
231 degradation in soil. For longer time points (up to day 28), the mass loss increased and reached
232 values similar to the one measured for untreated soil, probably indicating the inefficacy of the
233 sodium azide treatment in the long term. Biodegradation studies were also conducted in
234 untreated soil at 25°C and resulted in the complete biodegradation of LCC, MCC and HCC
235 materials in less than 30 days (Supplementary Fig. 7). Biodegradation in sterilized soil only
236 resulted in less than 50% of mass loss over a period of 30 days. The complete biodegradation
237 of the coating within the life cycle of the plant is an important feature to minimize the
238 environmental impact of agriculture and the release of pollutant in the soil. Recently,
239 policymakers have promoted new laws that strictly regulate the biodegradation of polymers
240 released in the environment for agricultural application. For example, in January 2018 the
241 European Chemicals Agency (ECHA) examined the need for an EU-wide restriction on the
242 use of intentionally added microplastic particles (IAMPs) in products placed on the EU
243 market, including food and agriculture, with non-biodegradable microplastics forecasted to be
244 banned in 2025[66].
245
246 Seedling germination and growth in semi-arid conditions
247 All together, these results suggest that the seed coating properties may be programmed by
248 varying several parameters including relative P:C concentration, amount of Ca^{2+} during
249 materials fabrication and presence of nutrients to design an environment that can support
250 resuscitation and growth of plant growth promoting rhizobacteria. In particular, for the
251 purpose of our study, we selected MCC as the hydrogel of choice to conduct germination
252 studies, given the combination of homogenous *R. tropici* CIAT 899 colonization, water
253 absorption and mechanical properties. In a preliminary study, germination of *P. vulgaris* seeds
254 was tested in a greenhouse setting by applying the following treatments: i) no treatment
255 (negative control), ii) inoculation with 3% poly(vinylpyrrolidone) (PVP) solution with *R.*

256 *tropici* CIAT 899-GFP (positive control), iii) bilayer seed coating with Layer 2 applied via
257 spray-coating, and iv) bilayer coating with Layer 2 applied via dip-coating. Seedlings were
258 checked for nodulations at day 14 after germination, to ensure successful delivery of
259 rhizobacteria and root colonization (Fig. 4b). A 100% nodulation rate was observed for all
260 three procedures where *R. tropici* CIAT 899 were added to the soil. Application of Layer 2
261 both via spray-coating and dip-coating resulted in roots that were more developed when
262 compared to the positive control, suggesting that the seed enhancement technology
263 outperforms current standard materials and can be applied with tools largely available by
264 growers.

265 To further test the efficacy of the two-layer coatings (L2) in mitigating environmental
266 stressors typical of semi-arid regions, we conducted germination studies at the UM6P
267 experimental farm in Ben Guerir, Morocco, using native soil (Fig. 4c). Soil analysis revealed
268 that a composition typical of sandy soils, slightly alkaline and prone to induce drought stress
269 due to limited water retention capacity. The soil was rich in nitrogen and phosphate and
270 concentrations of oligoelements such as manganese and zinc were sufficient, while there was
271 a slight deficiency in copper content (Supplementary Table 1). To investigated the
272 effectiveness of L2 to induce water-stress tolerance, we exposed L2-coated *P. vulgaris* seeds
273 to soils with a decreasing water potential (Ψs), by altering the watering conditions to induce
274 water stress regimes (Fig. 4c). Seeds with no coating (C) and seeds coated only with Layer 1
275 (L1) were used as control and one-way ANOVA test with Bonferroni's correction was used to
276 analyze the data collected. When comparing the different watering conditions in 150 g of soil
277 per plant, it was observed that for mild (Ψs = -12 kPa) and severe (Ψs = -20 kPa) water-
278 stressed conditions, L2 coating statistically significantly influenced germination and plant
279 health, when compared to the two controls. L2 seeds resulted in shoot dry mass that were
280 higher, respectively, when compared to C and L1 seeds for Ψs at -1kPa, -12 kPa and -20 kPa.

281 Shoot length was not a factor that seemed to be determined by coating maybe because this
282 was early on in the growth process. No statistical significant difference was found for shoot
283 length between L2, L1 and C seeds for Ψs = -20 kPa. It was also observed that root
284 architecture was significantly affected by seed and water treatments. Seeds germinated in soil
285 with Ψs = -1 kPa and Ψs = -5 kPa had the longest roots in comparison with seeds germinated
286 in water stress conditions, i.e. Ψs = -12 kPa and Ψs = -20 kPa. Under water stress regimes,
287 roots in L2 and L1 seeds were statistically significantly longer when compared to C seeds,
288 indicating that the coating treatments provided a better environment for early root
289 establishment. Measurement of chlorophyll content in leaves showed that watering regime
290 but not seed coating affected the production of the green pigment. Measurement of total
291 phenolic compounds (TPC) is correlated to drought stress as plants release phenolic
292 compounds to mitigate water deficit.[67] TPC was statistically significantly lower for L2 seeds
293 when compared to L1 and C seeds, indicating the contribution of the designed hydrogel to
294 induce water-stress tolerance. Measurement of stomatal conductance corroborated this
295 finding. *P. vulgaris* cultured in water stress regimes lower stomatal conductance to limit water
296 loss.[68] In our experiments, L2 seeds showed statistically significant higher stomatal
297 conductance for Ψs = -1 kPa, -5 kPa and -12 kPa, when compared to the L1 and C seeds and
298 a higher stomatal conductance for Ψs = -20 kPa to C seeds, indicating a better tolerance to
299 water deficiency. Altogether, these results indicate that the L2 coating positively influence
300 plant establishment of *P. vulgaris* in a semi-arid soil and under water stress.
301
302 **Discussion**
303 In this study we investigated the use of a biomaterials and drug delivery approach to engineer
304 a programmable seed coating technology for effective delivery and growth of rhizobacteria in
305 the spermosphere. Activated upon sowing, the two-layered coating technology enabled the

306 resuscitation and self-replication of rhizobia within a biopolymer-based hydrogel that
307 resembles seed mucilage and resulted in the formation of microbial colonies that formed
308 symbiotic nodules with plant roots and induced water stress tolerance in semi-arid conditions.
309 Furthermore, the use of biopolymers generally used in food gels provide a largely available,
310 cost-effective and non-toxic solution to mitigate abiotic stress. Together, these findings open
311 the door to the use of enhanced seed coating technologies to address specific weather and soil
312 conditions, to adapt agriculture to changes in climate patterns while also minimizing the use
313 of scarce and energy-intensive inputs.
314
315 Methods
316 *Materials*
317 Materials fabrication, hydration and dehydration studies are reported below. Extensive details
318 of the experimental procedures are reported in Supporting Information
319 *Hydrogel fabrication*: Four types of gels were prepared with different ratios of low-
320 methoxylated pectin (P) from citrus peel (> 74% galacturonic acid, > 6.7% methoxy groups,
321 Sigma-Aldrich, St. Louis, MO) to NaCMC (C) (molecular weight 90,000 g/mol, degree of
322 substitution 0.7, Sigma-Aldrich, St. Louis, MO). The tested P:C ratios were 1:0, 3:1, 1:1, and
323 1:3, but the total amount of polysaccharides was 5 wt% for all solutions. For the gel
324 preparation, monomeric sugars (D-(+)-xylose 20.9 mM , L-(+)-arabinose 6.28 mM, DL-
325 arabinose 6.28 mM, L-rhamnose 8.94 mM (Sigma-Aldrich, St. Louis, MO) with the ratio
326 30:9:9:14) were first added to deionized (DI) water to mimic the ratio found in Basil seeds[61].
327 After complete mixing of the polysaccharides in the sugar solution, three calcium chloride
328 ($CaCl_2$, Sigma-Aldrich, St. Louis, MO) concentrations were added to each mix from a 1 mM
329 $CaCl_2$ stock solution in DI water: HCC (15 mM), MCC (10 mM), and LCC (5 mM). After
330 leaving the solution for 24 hours, 70 mol% (mol percentage of polysaccharides) of OH- (from
331 2 M NaOH stock solution) was added to each gel, to increase the pH and lead to gelation,

332 according to the egg-box model.[69] 48 hours later, the samples were prepared and air-dried for
333 24 hours at RT. From those gels, the best P:C ratio was selected by analyzing both the water
334 content over time and the GC. Only materials with selected P:C ratio were then optimized (pH
335 and $CaCl_2$ concentrations). Indeed, because the pH is only important for pectin gelation and
336 not NaCMC, the added NaOH amount had to be adjusted: 70 mol% of galacturonic acid
337 (pectin's principal monomer) rather than 70 mol% of all polysaccharides. $CaCl_2$
338 concentrations subsequently needed to be increased for the mechanical integrity of the gel.
339 Finally, full characterization was only done for the materials with the selected P:C ratio.
340 *Hydration studies*
341 To understand the swelling kinetics of the selected hydrogels, a hydration study was
342 conducted in solution. Wet 100 mm mesh nylon tea bags (DulytekTM, Seattle, WA) after five
343 flicks and dry hydrogel samples (ten 3.5 mm punches, n = 3) were weighed (Mettler Toledo,
344 Greifensee, Switzerland). To measure the swelling, the gel punches were placed in the tea
345 bags in 154 mM NaCl solution (Sigma-Aldrich, St. Louis, MO) and their weights (punch +
346 bag) were repeatedly measured after 1 h, 3 h, 6 h, 12 h, 24 h, and 36 h. After each time point,
347 the bags with the punches were put back in solution. The swelling ratio (SR) was calculated as
348 follows: SR = (Ws - Wi) / Wi * 100, with Ws being the weight of the swollen samples at the
349 different time points and Wi being the initial weight of the dried sample before the
350 experiment. Ws was calculated as the mass of the wet tea bag with the wet sample minus the
351 weight of the wet tea bag. Another hydration study was then conducted in soil (African
352 Violet Potting Mix, Scotts Miracle-Gro, OH) to highlight the effect and interaction of
353 compressional soil forces vs. hydrogel swelling forces. Dried punches of each gel (8 mm
354 diameter, n = 3) were put in 100 mm mesh nylon tea bags. Dried punches were weighed
355 beforehand. Samples in bags were buried in the soil at three different moisture conditions
356 (hydrated with deionized water): 10%, 25%, and 50% over a 24-hour period. Hydration was
357 monitored with a hydrometer (Soil Moisture Sensor and LabQuest mini, Vernier, Beaverton,

358 OR). Then, tea bags were taken out and cut to retrieve the wet punches, which were weighed.
359 Their SR was finally calculated according to the SR equation previously described.

360 *Dehydration*

361 Dry hydrogel samples (ten 3.5 mm punches per sample, n = 5), as well as wet and dry 100
362 mm mesh nylon tea bags, were weighed. Dried samples (Wi) were put in the tea bags and
363 immersed in 154 mM NaCl solution for 12 hours. Teabags containing the samples were then
364 retrieved from the water and flicked five times before being weighed to determine the SR as
365 described above. Samples were then let to air-dry at RT. From there on, weight was measured
366 every hour (Ws) until the samples were dry to obtain a water content curve (changes in SR
367 over time). Ws was calculated as the mass of the teabag with the sample minus the weight of
368 the teabag (wet weight for the first hour and then dry weight). The pH of the 154 mM NaCl
369 solution in which the bagged samples were swollen was measured after 12 hours with a pH
370 meter (Orion Dual Star, ThermoFisher Scientific, Waltham, MA).

371 *Gel content*

372 The dry weight of 8 mm hydrogel punches (n = 3) was measured before immersing them in
373 154 mM NaCl solution for 12 hours (W_i). The samples were then air-dried for 24 hours at RT
374 and their weight measurement was taken again (W_d). The gel content (GC) was calculated as
375 follows[70,71] :

376 $$GC = \frac{W_d}{W_i} \cdot 100 \qquad (2)$$

377 with W_i being the initial dry weight of the gel and W_d corresponding to the weight of the dried
378 sample after swelling and deswelling the initial dry sample.

379 *Macro and micromorphology*

380 To have a visual sense of the swelling volume and integrity of the selected hydrogels, pictures
381 of 8 mm punches were taken in the dry state and after being swelled in 154 mM NaCl solution
382 for 12 hours (camera D3400, Nikon, Tokyo, Japan). Pictures were analyzed with ImageJ

383 software available from https://imagej.nih.gov/ij/ (National Institutes of Health, MD). The
384 volumes of the gels were calculated by measuring (*1*) the diameter of each gel in the dry and
385 wet states at four different angles (0°, 45°, 90°, and 125°) and (*2*) the height of each gel in the
386 dry and wet states at three spots (on each end and in the middle). The volume variation (VV)
387 was calculated with the following equation:

388 $$VV = \frac{V_s - V_i}{V_i} \cdot 100 \qquad (3),$$

389 with V_i being the initial dry volume of the hydrogel and V_s being the swollen volume of the
390 gel after 12 hours of immersion in 154 mM NaCl solution.
391 To visualize the microstructure of the hydrogels, 8 mm punches were swollen in 154 mM
392 NaCl solution for 12 hours. Small pieces 2-3 mm were places in planchets at room
393 temperature and plunged into liquid nitrogen. The frozen planchets were kept cold and
394 transferred into a ACE900 freeze fracture machine. Samples were fractured, revealing the interior,
395 then shadowed with 2 nm of platinum and coated with 10 nm of carbon. Coated samples were
396 imaged directly in the Zeiss Crossbeam 540 FIB/SEM (Thornwood, NY) fitted with a Leica
397 cryostage while held at below -150˚C. The LCC and MCC samples were soaked in 20% glycerol,
398 a cryoprotectant for 30 minutes to prevent ice formation prior to freezing.
399 *Mechanical properties*
400 To evaluate the strength of wet samples, non-confined compression tests were conducted
401 (5943 Instron, Norwood, MA) on round gel samples (n = 3, diameter 38 mm, thickness 16
402 mm). The strain speed rate was set to 100% min^{-1}, and the whole experiment was filmed, until
403 a strain compression of 30%. Tangents to all compressive stress-strain curves were calculated
404 at 5% strain, 10% strain, and 15% strain, to evaluate which tangents were fitting the best the
405 linear (elastic) regions of each gel type.
406 *Nanoindentation*: Nanoindentaion measurements were performed on a Hysitron TriboIndenter
407 with a nanoDMA transducer (Bruker, Billerica, MA). Samples were indented in load control
408 mode with a peak force of 500 μN and a standard load-peak hold-unload function. Reduced

409 modulus was calculated by fitting the unloading data (with upper and lower limits being 95%
410 and 20%, respectively) using the Oliver-Pharr method and converted to Young's modulus
411 assuming a Poisson's ratio of 0.33 for all samples. Each type of sample was prepared and
412 indented in triplets to ensure good fabrication repeatability. For each sample, indentation was
413 performed at 3 locations a total of 36 points (6×6 grid with an increment of 20 μm in both
414 directions) at each location to ensure statistical reliability of the modulus measurements.
415 *Bacterial growth*
416 To assess bacterial growth in the presence of the selected hydrogels, two experiments were
417 conducted. For both, a growth media was prepared by mixing 5 g of BactoTM Peptone (BD
418 Biosciences, Franklin Lakes, NJ), 3 g of yeast extract (Sigma-Aldrich, St. Louis, MO), and 10
419 mL of 0.7 M $CaCl_2$ solution to 1L of DI water. The following antibiotics (Sigma-Aldrich, St.
420 Louis, MO) were then added: Rifampicin (25 mg/mL), Nalidixic acid (20 mg/mL), and
421 Tetracycline (10 mg/mL). The media was sterilized by autoclaving for 50 minutes at 120°C.
422 *R. tropici* CIAT 899 was grown in media overnight (28˚C, 250 rpm) in 14 mL falcon round-
423 bottom tubes (Corning Inc., Corning, NY). The tubes were then centrifuged at 4200 rpm for
424 10 minutes (5910 R, Eppendorf, Hauppauge, NY) and the bacterial pellets were resuspended
425 in 5 mL PBS (BupHTM phosphate-buffered saline packs, ThermoFisher Scientific, Waltham,
426 MA). The OD600 was finally adjusted to 0.1 before the following two experiments were
427 performed.
428 Experiment 1: Two MCC gels were fabricated, one with the usual basil-inspired
429 monosaccharides and one with the same amount of sucrose instead. Because it is known that
430 *R. tropici* CIAT 899 can digest sucrose, this experiment would thus give information about
431 the bacteria digestion of basil sugars. 48 hours after the NaOH addition, twelve square
432 hydrogel samples (1 cm^3) were cut out and air-dried for 24 hours at RT. The gels were then
433 rehydrated in PBS for 12 hours in 15 mL tubes. For controls (n = 3), the PBS was renewed,
434 and for positive samples (n = 3), the initial PBS was replaced by PBS with *R. tropici* CIAT

435 899 (OD600 = 0.1). *R. tropici* CIAT 899 synthesizing green fluorescent protein (*R. tropici*
436 CIAT 899-GFP)[62,72] were used to conduct hydrogel colonization studies. GFP fluorescence
437 intensity of the solution was repeatedly measured at the following time points: 5 h, 8 h, 24 h,
438 30 h, 36 h, and 48 h (Safire2, Tecan, Switzerland). The excitation light was 491 nm, the
439 emission light was 530 nm, and the gain was set to 70. GFP fluorescent intensity gave
440 information on the amount of the fluorescent reporter expressed by *R. tropici* CIAT 899-GFP
441 and it was used as an indication of living bacteria and their growth.
442 Experiment 2: The fluorescence experiment was repeated with the three P:C 1:1 gels (LCC,
443 MCC, and HCC). The time points at which fluorescence was repeatedly measured were 2 h, 4
444 h, 6 h, 9 h, 15 h, 24 h, 27 h, 30 h, 33 h, 39 h, and 48 h.
445 *Histological sections*
446 To determine if bacteria were attracted by the hydrogel and migrated inside them, pieces of
447 hydrogels were retrieved after 6 and 54 hours of incubation with *R. tropici* CIAT 899-GFP,
448 and fixed in 10% formalin (Sigma-Aldrich, St. Louis, MO) for 18 hours, washed twice with
449 PBS, and casted into HistoGelTM (ThermoFisher Scientific, Waltham, MA). Distinct samples
450 were used per each time point considered. After thirty minutes, two slices were cut out from
451 the sample and placed in a cassette in formalin for an additional hour. Finally, all gels were
452 conserved in 70% ethanol before being brought for histology (Gram-negative staining, Hope
453 Babette Tang Histology Facility, Koch Institute, MIT, MA).
454 *Migration studies*: 1% (w/v) 45 minute-boiled silk fibroin aqueous solution was prepared
455 from silkworm cocoons (Tajima Shoji Co., LTD., Yokohama, Japan) as described in
456 Rockwood et al.[39]and mixed with a 1% (w/v) aqueous solution of trehalose (D-(+)-trehalose
457 anhydrous, TCI Chemicals, Tokyo, Japan). The two solutions were added together to a final
458 silk:trehalose ratio of 1:3. *R. tropici* CIAT 899-GFP were centrifuged at 4200 rpm for 10
459 minutes (Eppendorf 5910 R, Hamburg, Germany) and the pellet was resuspended in the
460 silk:trehalose solution until an OD600 of 0.1 was reached. 50 mL of this solution was drop-

461 casted on a PDMS sheet and air-dried for 48 hours at RT to form a film. In the meantime, the
462 three P:C 1:1 gels were prepared as explained earlier. Right after the addition of NaOH, each
463 viscous solution was transferred to the inserts of a 12-transwell plate (Corning Inc., Corning,
464 NY) (n = 4) to reach a height of 2 mm. The gels were finally air-dried for 48 hours at RT. On
465 top of the dried gel, a dry film was deposited on Day 0. At the bottom of the transwell plate,
466 PBS was added so that only the bottom of the gel touched the solution through the permeable
467 membrane. One sample of each gel was taken out on day 1, day 3, and day 7, i.e. distinct
468 samples were used per each time point considered. The samples were fixed with 10%
469 formalin solution for 30 minutes (Sigma-Aldrich, St. Louis, MO) and incubated with the
470 TrueVIEWTM kit (Vector Laboratories, CA) for 5 minutes to quench the autofluorescence of
471 the hydrogels. A cross-section of each gel was then imaged with a confocal microscope
472 (inverted Ti Nikon1AR ultra-fast spectral scanning confocal microscope, Nikon Tokyo,
473 Japan) at each time point to observe the migration of the microbes across the hydrogel. All
474 images were taken with the exact same parameters. The fluorescent images were then
475 processed with the ImageJ software to obtain a maximum intensity Z-projection.
476 *Diffusion studies*
477 To compare the diffusion of nutrients through hydrogels, 4-mL solutions of LCC, MCC and
478 HCC hydrogel were prepared and added to 5-mL tubes and solidified for 48 hours. Gels were
479 then hydrated in 154 mM NaCl solution for 24 hours before the diffusion study. 1 mL of a
480 solution of fluorescein (100 mM) in water was pipetted on top of each hydrogel and the gels
481 were photographed every 10 minutes for 150 minutes. The distance the fluorophore had
482 traveled was measured at each time point and these data were used to calculate the diffusion
483 rate of small molecules through the hydrogel[63]. Samples were measured repeatedly for time
484 points considered.
485 *Material biodegradation*

486 Degradation of hydrogels in soil was evaluated over a one-month period. Dry samples of each
487 gel (five 8 mm punches, n = 3) were weighed beforehand (Wi). The samples in 100 mm mesh
488 tea bags were buried in 25% hydrated soil. 50 mL silk films containing *R. tropici* CIAT 899
489 (OD600 = 0.1) were prepared as explained above and one film was added to each tea bag. The
490 moisture condition of the soil was monitored with a hydrometer and DI water was added
491 when needed to maintain the 25% humidity level (5 mL every three days). A sample of each
492 gel was taken out on days 1, 3, 7, 14, and 28 (measurements were then taken from distinct
493 samples). They were quickly washed in 154 mM NaCl solution and then air-dried for 24
494 hours at RT before their weight was measured (W_d). Degraded gel (DG) amount was
495 calculated as described in equation (4):

496 $$DG = \frac{W_i - W_d}{W_i} \cdot 100 \qquad (4)$$

497 where, W_i is the initial dry weight of the sample and W_d the dry weight of the samples after
498 some time in PBS and bacteria or in soil, depending on the experiment. To investigate the
499 effects of a reduced microbial activity on the material biodegradation, 2% sodium azide
500 solution was mixed with the soil (1 ml per 1 g of soil)[73]. Biodegradation studies were
501 conducted at 16°C and 24°C.

502 *Rheology*: Isothermal gelation studies were conducted with a TA Instruments (New Castle,
503 DE) stress-controlled AR-G2 rheometer with a 40 mm, 2∞ cone-and-plate fixture at 25°C.
504 NaOH was added to the polymer mixture to induce bond formation (time t = 0) then
505 immediately transferred onto just rheometer plate, and measurement started at t = 60-90 s. For
506 time sweeping tests, storage moduli G′ and loss moduli G″ were monitored as a function of
507 time at a 1 Hz frequency and a 2% stress strain under constant temperature (25°C).

508 *Fluorescence Calibration*

509 To convert all fluorescence intensity numbers to OD600 values, a calibration curve was made.
510 *R. tropici* CIAT 899 were diluted in PBS at seven different OD600: 0, 0.1, 0.3, 0.5, 0.7, 1, and

511 1.1. The corresponding fluorescence intensities were measured and plotted against the
512 OD600. The excitation light was 491 nm, the emission light was 530 nm, and the gain was set
513 to 70. A linear model was fitted with MATLAB (R2018a, MathWorks, Natick, MA).

514 *Statistical Analysis*

515 Statistical analysis was performed on SRs, GCs, Es, and DGs with MATLAB (R2018a, Math-
516 Works, Natick, MA). Normality of the data was verified using the Jarque-Bera test. A One-
517 Way ANOVA test was applied, followed by pairwise comparison testing if the results showed
518 a statistically significant difference between the groups ($p<0.05$). Bonferroni's correction was
519 applied to counter the effects of multiple comparisons.

520 *Seed coating*: *P. vulgaris* seeds were surface sterilized with 10% bleach for 3 minutes, rinsed
521 in H_2O three times, and left to air dry. 80 mL of *R. tropici* CIAT 899-GFP (OD600 = 1) was
522 centrifuged at 4200 rpm in an Eppendorf centrifuge 5910 R (Hamburg, Germany). The
523 supernatant was discarded and 8 mL of dry 6 wt% silk fibroin-trehalose (1:3) solution was
524 added to the spun down *R. tropici* CIAT 899-GFP. Air-dried seeds were then dipped into this
525 solution for 120 seconds, taken out and left to dry (*Layer 1*). After slightly drying, the seeds
526 were either dip-coated into a hydrogel gelation solution just after adding NaOH and left to dry
527 (*Layer 2 dip*) or slightly sprayed with the hydrogel solution (*Layer 2 spray*). After drying, the
528 seeds were planted at the 24-hour mark.

529 *Growth conditions*

530 Initial assessment of seed growth and nodulation was carried out in African Violet soil.
531 Germination of *P. vulgaris* seeds was tested in a greenhouse setting by applying the following
532 treatments: i) no treatment (negative control), ii) inoculation with 3% poly(vinylpyrrolidone)
533 (PVP) solution with *R. tropici* CIAT 899-GFP (positive control), iii) bilayer seed coating with
534 Layer 2 applied via spray-coating, and iv) bilayer coating with Layer 2 applied via dip-
535 coating[74,75]. Seedlings were checked for nodulations at day 14 after germination, to ensure
536 successful delivery of rhizobacteria and root colonization. N=18 seeds per treatment were

537 used. Additionally, no statistically significant changes in soil electrical conductivity (EC)
538 were measured in soil where coated and uncoated seeds have germinated (2.13±0.03 and
539 2.12±0.02 mS/cm, respectively), indicating that the ions present in the coating do not
540 significantly affect EC.
541 Following this preliminary assessment, seed growth was carried out in semi-arid soil at UM6P
542 experimental farm in Ben Guerir, Morocco. Watering conditions were adjusted to obtain soils
543 with an average water potential (Ψs) of -1kPa, -5 kPa, -12 kPa and -20kPa over a 48 hour
544 time interval. Mild and severe water stress growth condition corresponded to Ψs = -12 kPa
545 and -20kPa, respectively. Soil tensiometers were made from a ceramic cup connected to an
546 acrylic glass tube and has a 136PC15G1 bridge pressure sensor (Micro Switch, Freeport, Il,
547 USA) on the top to measure the pressure inside the tubing caused by water dynamics between
548 the soil and water filled tube.) Tensiometers were used for each treatment in three replicates
549 to monitor the water potential. Lost water through evapotranspiration was replenished to
550 maintain the desired water potential. Healthy seeds from each treatment were evenly
551 germinated on plastic trays of 10 cm containing 150 g of a substrate mixture composed by
552 30% of sieved sand (2 mm) and topsoil, manually shifted from stone. After adding water
553 treatment solution to each replicate, trays were placed in the growth chamber, where relative
554 humidity was 65 to 70%, night temperature 16˚C and day temperature 24˚C and photoperiod
555 was 16/8 h. All the treatments were laid out in a completely randomized design, replicated
556 five times, and kept for recording physiological attributes. To find out the role of seed
557 coating in alleviating drought stress and to evaluate the effect on plant establishment and
558 behavior along the growth cycle, three random seedlings were transplanted to large pots
559 (30/20 cm), 20 days after sowing. Pots, containing 4 kg of the substrate mixture, were kept
560 under the greenhouse to allow roots and appropriate leaves development. Irrigation was
561 applied following the same water treatments used before. Different measurements from

562 distinct samples were taken to investigate the treatment general effects: (*1*) Shoot length over
563 time; (*2*) Shoot dry weight; (3) Root length measured with WinRhizo (Regent Instruments
564 Inc., Quebec City, Canada) root scanner; (4) Stomatal conductance was measured using a SC-
565 1 Leaf Porometer (Decagon Devices, Inc. USA); (*5*) Chlorophyll content was measured with
566 a the CL-01 Chlorophyll Content System (Hansatech Instruments Ltd, Norfolk, England); (*6*)
567 Total Phenolic Compounds (TPC) was measured by grounding in a mortar containing 5 ml of
568 50% ethanol solution fragments of leaves and roots (0.5 g FM). The extracts were collected in
569 tubes with lids and labelled, then left in the refrigerator overnight. Upon adding 0.5 ml of
570 chloroform in 3 ml of extract, tubes were vortexed and centrifuged for 5 min at 5,000 rpm.
571 TCP assay was performed using the Folin-Ciocalteu reagent.[76] Briefly, 0.5 ml of extract, 3 ml
572 of distilled water and 0.5 ml of Na_2CO_3 (20%) were mixed in a test tube. After 3 minutes, 0.5
573 ml of Folin-Ciocalteu reagent was added. The test tubes were left for 30 min at 40°C before
574 measuring absorbance at 760 nm. The content of phenolic compounds was calculated using
575 gallic acid for the standard curve and expressed in milligrams per gram of fresh leaf matter.
576

577 Acknowledgements
578 We acknowledge Miguel Lara for *R. tropici* CIAT 899-GFP from Universidad Nacional
579 Autonoma de Mexico. This work was partially supported by Office of Naval Research
580 (Award No. N000141812258), the National Science Foundation (Award No. CMMI-
581 1752172), the MIT Paul M. Cook Career Development Professorship. The authors
582 acknowledge OCP S.A. and Université Mohammed VI Polytechnique-MIT Research
583 Program.
584
585 **Data availability**
586 All relevant data are included in the paper and/or its Supplementary Information. All raw data
587 are available from the authors on request.

Contributions

A.T.Z., J.L., M.M., B.M. and L.K. designed the study. A.T.Z., J.L., M.M., H.S., S.M., D.K. and H.M.E.F. collected and analyzed the data. All authors contributed to the discussion and interpretation of the results. The manuscript was drafted by A.T.Z., L.L., H.S., M.M, L.K and B.M. and reviewed and approved by the other authors.

Corresponding Author

Benedetto Marelli – bmarelli@mit.edu

Ethics declarations

N/A

Competing interests

B.M and A.T.Z. are co-inventors in a patent application that describes the coating technology reported in this study. BM is co-founder of Mori, Inc, a company that develops silk-based edible coatings to extend the shelf-life of food.

Supplementary Information

Supplementary Figs. 1–7

Supplementary Table 1

References

1. Lesk, C., Rowhani, P. & Ramankutty, N. Influence of extreme weather disasters on global crop production. *Nature* **529**, 84–87 (2016).
2. Mendoza-Suárez, M. A. *et al.* Optimizing Rhizobium-legume symbioses by simultaneous measurement of rhizobial competitiveness and N2 fixation in nodules. *Proc. Natl. Acad. Sci. U. S. A.* **117**, 9822–9831 (2020).
3. Steinwand, M. A. & Ronald, P. C. Crop biotechnology and the future of food. *Nat. Food* **1**, 273–283 (2020).
4. Gilbertson, L. M. *et al.* Guiding the design space for nanotechnology to advance sustainable crop production. *Nat. Nanotechnol.* **15**, 801–810 (2020).
5. Kah, M., Tufenkji, N. & White, J. C. Nano-enabled strategies to enhance crop nutrition and protection. *Nat. Nanotechnol.* (2019). doi:10.1038/s41565-019-0439-5
6. Eleftheriadou, M., Pyrgiotakis, G. & Demokritou, P. Nanotechnology to the rescue: using nano-enabled approaches in microbiological food safety and quality. *Curr. Opin. Biotechnol.* **44**, 87–93 (2017).
7. Xu, T. *et al.* Enhancing Agrichemical Delivery and Seedling Development with Biodegradable, Tunable, Biopolymer-Based Nanofiber Seed Coatings. *ACS Sustain. Chem. Eng.* **8**, 9537–9548 (2020).
8. Farias, B. V. *et al.* Electrospun Polymer Nanofibers as Seed Coatings for Crop Protection. *ACS Sustain. Chem. Eng.* **7**, 19848–19856 (2019).
9. Glick, B. R. Introduction to Plant Growth-Promoting Bacteria. in *Beneficial Plant-Bacterial Interactions* 1–37 (Springer International Publishing, 2020). doi:10.1007/978-3-030-44368-9_1
10. Tian, H. *et al.* A comprehensive quantification of global nitrous oxide sources and sinks. *Nature* **586**, 248–256 (2020).
11. Food and Agriculture Organization of the United Nations. *Status of the World's Soil*

Resources. (2015).

12. Ricciardi, V. *et al.* A scoping review of research funding for small-scale farmers in water scarce regions. *Nat. Sustain.* **3**, 836–844 (2020).

13. Food and Agriculture Organization of the United Nations. *The State of Food Security and Nutrition in the World*. 214 (2019).

14. Behera, S. & Mahanwar, P. A. Superabsorbent polymers in agriculture and other applications: a review. *Polym. Technol. Mater.* **59**, 341–356 (2020).

15. Zhao, C., Zhang, M., Liu, Z., Guo, Y. & Zhang, Q. Salt-Tolerant Superabsorbent Polymer with High Capacity of Water-Nutrient Retention Derived from Sulfamic Acid-Modified Starch. *ACS omega* **4**, 5923–5930 (2019).

16. Beigi, S., Azizi, M. & Iriti, M. Application of Super Absorbent Polymer and Plant Mucilage Improved Essential Oil Quantity and Quality of Ocimum basilicum var. Keshkeni Luvelou. *Molecules* **25**, 2503 (2020).

17. Stahl, J. D., Cameron, M. D., Haselbach, J. & Aust, S. D. Biodegradation of superabsorbent polymers in soil. *Environ. Sci. Pollut. Res.* **7**, 83–88 (2000).

18. Niu, X., Song, L., Xiao, Y. & Ge, W. Drought-Tolerant Plant Growth-Promoting Rhizobacteria Associated with Foxtail Millet in a Semi-arid Agroecosystem and Their Potential in Alleviating Drought Stress. *Front. Microbiol.* **8**, 2580 (2018).

19. Kuypers, M. M. M., Marchant, H. K. & Kartal, B. The microbial nitrogen-cycling network. *Nat. Rev. Microbiol.* **16**, 263–276 (2018).

20. Trivedi, P., Leach, J. E., Tringe, S. G., Sa, T. & Singh, B. K. Plant–microbiome interactions: from community assembly to plant health. *Nat. Rev. Microbiol.* **18**, 607–621 (2020).

21. Dodd, I. C. & Pé Rez-Alfocea, F. Microbial amelioration of crop salinity stress. *J. Exp. Bot.* **63**, 3415–3428 (2012).

22. O'Callaghan, M. Microbial inoculation of seed for improved crop performance: issues

and opportunities. *Appl. Microbiol. Biotechnol.* **100**, 5729–5746 (2016).

23. Zhou, X. *et al.* Microbiota in the Rhizosphere and Seed of Rice From China, With Reference to Their Transmission and Biogeography. *Front. Microbiol.* **11**, 995 (2020).

24. Gou, J. Y. *et al.* Biofertilizers with beneficial rhizobacteria improved plant growth and yield in chili (Capsicum annuum L.). *World J. Microbiol. Biotechnol.* **36**, 86 (2020).

25. Enebe, M. C. & Babalola, O. O. The influence of plant growth-promoting rhizobacteria in plant tolerance to abiotic stress: a survival strategy. *Appl. Microbiol. Biotechnol.* **102**, 7821–7835 (2018).

26. Santos, M. S., Nogueira, M. A. & Hungria, M. Microbial inoculants: reviewing the past, discussing the present and previewing an outstanding future for the use of beneficial bacteria in agriculture. *AMB Express* **9**, (2019).

27. Jansson, J. K. & Hofmockel, K. S. Soil microbiomes and climate change. *Nat. Rev. Microbiol.* **18**, 35–46 (2020).

28. Soumare, A. *et al.* Exploiting Biological Nitrogen Fixation: A Route Towards a Sustainable Agriculture. *Plants (Basel, Switzerland)* **9**, 1011 (2020).

29. McIntyre, H. J. *et al.* Trehalose Biosynthesis in Rhizobium leguminosarum bv. trifolii and Its Role in Desiccation Tolerance. *Appl. Environ. Microbiol.* **73**, 3984 LP – 3992 (2007).

30. Vriezen, J. A., de Bruijn, F. J. & Nüsslein, K. R. Desiccation induces viable but Non-Culturable cells in Sinorhizobium meliloti 1021. *AMB Express* **2**, 6 (2012).

31. Geetha, S. J. & Joshi, S. J. Engineering rhizobial bioinoculants: a strategy to improve iron nutrition. *Sci. World J.* 315890 (2013). doi:10.1155/2013/315890

32. Molina-Romero, D. *et al.* Compatible bacterial mixture, tolerant to desiccation, improves maize plant growth. *PLoS One* **12**, (2017).

33. Teixeira, A., Iannetta, P., Binnie, K., Valentine, T. A. & Toorop, P. Myxospermous seed-mucilage quantity correlates with environmental gradients indicative of water-

deficit stress: Plantago species as a model. *Plant Soil* **446**, 343–356 (2020).

34. Western, T. L. The sticky tale of seed coat mucilages: Production, genetics, and role in seed germination and dispersal. *Seed Science Research* **22**, 1–25 (2012).

35. Kreitschitz, A. & Gorb, S. N. The micro- and nanoscale spatial architecture of the seed mucilage-Comparative study of selected plant species. *PLoS One* **13**, e0200522–e0200522 (2018).

36. Phan, J. L. & Burton, R. A. New Insights into the Composition and Structure of Seed Mucilage. *Annual Plant Reviews online* 63–104 (2018). doi:doi:10.1002/9781119312994.apr0606

37. Sun, H. & Marelli, B. Growing silk fibroin in advanced materials for food security. *MRS Commun.* 1–15 (2021). doi:10.1557/s43579-020-00003-x

38. Zhou, Z. *et al.* Engineering the Future of Silk Materials through Advanced Manufacturing. *Adv. Mater.* **30**, 1706983 (2018).

39. Rockwood, D. N. *et al.* Materials fabrication from Bombyx mori silk fibroin. *Nat. Protoc.* **6**, 1612–1631 (2011).

40. Marelli, B., Brenckle, M. A., Kaplan, D. L. & Omenetto, F. G. Silk Fibroin as Edible Coating for Perishable Food Preservation. *Sci. Rep.* **6**, 0–1 (2016).

41. Marelli, B. *et al.* Programming function into mechanical forms by directed assembly of silk bulk materials. *Proc. Natl. Acad. Sci. U. S. A.* **114**, 451–456 (2017).

42. Kim, D. *et al.* A Microneedle Technology for Sampling and Sensing Bacteria in the Food Supply Chain. *Adv. Funct. Mater.* **31**, 2005370 (2021).

43. Cao, Y., Lim, E., Xu, M., Weng, J. K. & Marelli, B. Precision Delivery of Multiscale Payloads to Tissue-Specific Targets in Plants. *Adv. Sci.* **7**, 1903551 (2020).

44. Sun, H. & Marelli, B. Polypeptide templating for designer hierarchical materials. *Nat. Commun.* **11**, 351 (2020).

45. Pritchard, E. M. & Kaplan, D. L. Silk fibroin biomaterials for controlled release drug

delivery. *Expert Opin. Drug Deliv.* **8**, 797–811 (2011).

46. Crowe, J. H., Carpenter, J. F. & Crowe, L. M. The role of vitrification in anhydrobiosis. *Annu. Rev. Physiol.* **60**, 73–103 (1998).

47. Boothby, T. C. *et al.* Tardigrades Use Intrinsically Disordered Proteins to Survive Desiccation. *Mol. Cell* **65**, 975-984.e5 (2017).

48. Zvinavashe, A. T., Lim, E., Sun, H. & Marelli, B. A bioinspired approach to engineer seed microenvironment to boost germination and mitigate soil salinity. *Proc. Natl. Acad. Sci. U. S. A.* **116**, 25555–25561 (2019).

49. Vílchez, S., Tunnacliffe, A. & Manzanera, M. Tolerance of plastic-encapsulated Pseudomonas putida KT2440 to chemical stress. *Extremophiles* **12**, 297–299 (2008).

50. Cao, Y. & Mezzenga, R. Design principles of food gels. *Nat. Food* **1**, 106–118 (2020).

51. Redondo-Nieto, M., Wilmot, A. R., El-Hamdaoui, A., Bonilla, I. & Bolaños, L. Relationship between boron and calcium in the N 2 -fixing legume-rhizobia symbiosis. *Plant. Cell Environ.* **26**, 1905–1915 (2003).

52. Yoshimura, T., Sengoku, K. & Fujioka, R. Pectin-based surperabsorbent hydrogels crosslinked by some chemicals: Synthesis and characterization. *Polym. Bull.* **55**, 123–129 (2005).

53. Li, B. *et al.* Synthesis, characterization, and antibacterial activity of cross-linked chitosan-glutaraldehyde. *Mar. Drugs* **11**, 1534–1552 (2013).

54. Sehmi, S. K., Allan, E., MacRobert, A. J. & Parkin, I. The bactericidal activity of glutaraldehyde-impregnated polyurethane. *Microbiologyopen* **5**, 891–897 (2016).

55. Pathak, V. & Ambrose, R. P. K. Starch-based biodegradable hydrogel as seed coating for corn to improve early growth under water shortage. *J. Appl. Polym. Sci.* **137**, 48523 (2020).

56. Ahn, S. & Lee, S. J. Nano/Micro Natural Patterns of Hydrogels against Water Loss. *ACS Appl. Bio Mater.* **3**, 1293–1304 (2020).

57. Bakholdin, B. V. & Chashchikhina, L. P. Determination of the compression modulus of soils from compression-test data for calculation of pile-foundation settlements. *Soil Mech. Found. Eng.* **36**, 9–12 (1999).

58. Nataraj, M. S. & McManis, K. L. Strength and Deformation Properties of Soils Reinforced With Fibrillated Fibers. *Geosynth. Int.* **4**, 65–79 (1997).

59. Taylor, A. G. *et al.* Seed enhancements. *Seed Sci. Res.* **8**, 245–256 (1998).

60. Li, J. & Mooney, D. J. Designing hydrogels for controlled drug delivery. *Nat. Rev. Mater.* **1**, 1–17 (2016).

61. Samateh, M. *et al.* Unravelling the secret of seed-based gels in water: The nanoscale 3D network formation. *Sci. Rep.* **8**, (2018).

62. Nanjareddy, K. *et al.* Nitrate regulates rhizobial and mycorrhizal symbiosis in common bean (*Phaseolus vulgaris* L.). *J. Integr. Plant Biol.* **56**, 281–298 (2014).

63. Yin, N. *et al.* Bacterial cellulose as a substrate for microbial cell culture. *Appl. Environ. Microbiol.* **80**, 1926–32 (2014).

64. Kandemir, N., Vollmer, W., Jakubovics, N. S. & Chen, J. Mechanical interactions between bacteria and hydrogels. *Sci. Rep.* **8**, 10893 (2018).

65. Lichter, J. A. *et al.* Substrata mechanical stiffness can regulate adhesion of viable bacteria. *Biomacromolecules* **9**, 1571–1578 (2008).

66. *ECHA: Restricting the Use of Intentionally Added Microplastic Particles to Consumer or Professional Use Products of Any Kind-ANNEX XV RESTRICTION REPORT*. (2019).

67. Mansori, M. *et al.* Seaweed extract effect on water deficit and antioxidative mechanisms in bean plants (Phaseolus vulgaris L.). *J. Appl. Phycol.* **27**, 1689–1698 (2015).

68. Beebe, S. E., Rao, I. M., Blair, M. W. & Acosta-Gallegos, J. A. Phenotyping common beans for adaptation to drought. *Front. Physiol.* **4**, 35 (2013).

69. Tho, I., Sande, S. A. & Kleinebudde, P. Cross-linking of amidated low-methoxylated pectin with calcium during extrusion/spheronisation: Effect on particle size and shape. in *Chemical Engineering Science* **60**, 3899–3907 (Pergamon, 2005).

70. Silva, H. *et al.* Effect of water availability on growth and water use efficiency for biomass and gel production in Aloe Vera (Aloe barbadensis M.). *Ind. Crops Prod.* **31**, 20–27 (2010).

71. Yacob, N. & Hashim, K. Morphological effect on swelling behaviour of hydrogel Synthesis of chemical cross-linked gelatin hydrogel reinforced with cellulose nanocrystals (CNC) AIP Conference Morphological Effect on Swelling Behaviour of Hydrogel. *Swelling J. Chem. Phys.* **1584**, 521 (2014).

72. Nanjareddy, K. *et al.* A legume TOR protein kinase regulates Rhizobium symbiosis and is essential for infection and nodule development. *Plant Physiol.* **172**, 2002–2020 (2016).

73. Trevors, J. T. Sterilization and inhibition of microbial activity in soil. *J. Microbiol. Methods* **26**, 53–59 (1996).

74. Deaker, R., Roughley, R. J. & Kennedy, I. R. Legume seed inoculation technology—a review. *Soil Biol. Biochem.* **36**, 1275–1288 (2004).

75. Mukhtar, S., Shahid, I., Mehnaz, S. & Malik, K. A. Assessment of two carrier materials for phosphate solubilizing biofertilizers and their effect on growth of wheat (Triticum aestivum L.). *Microbiol. Res.* **205**, 107–117 (2017).

76. Hazzoumi, Z., Moustakime, Y., hassan Elharchli, E. & Joutei, K. A. Effect of arbuscular mycorrhizal fungi (AMF) and water stress on growth, phenolic compounds, glandular hairs, and yield of essential oil in basil (Ocimum gratissimum L). *Chem. Biol. Technol. Agric.* **2**, 1–11 (2015).

Fig. 1

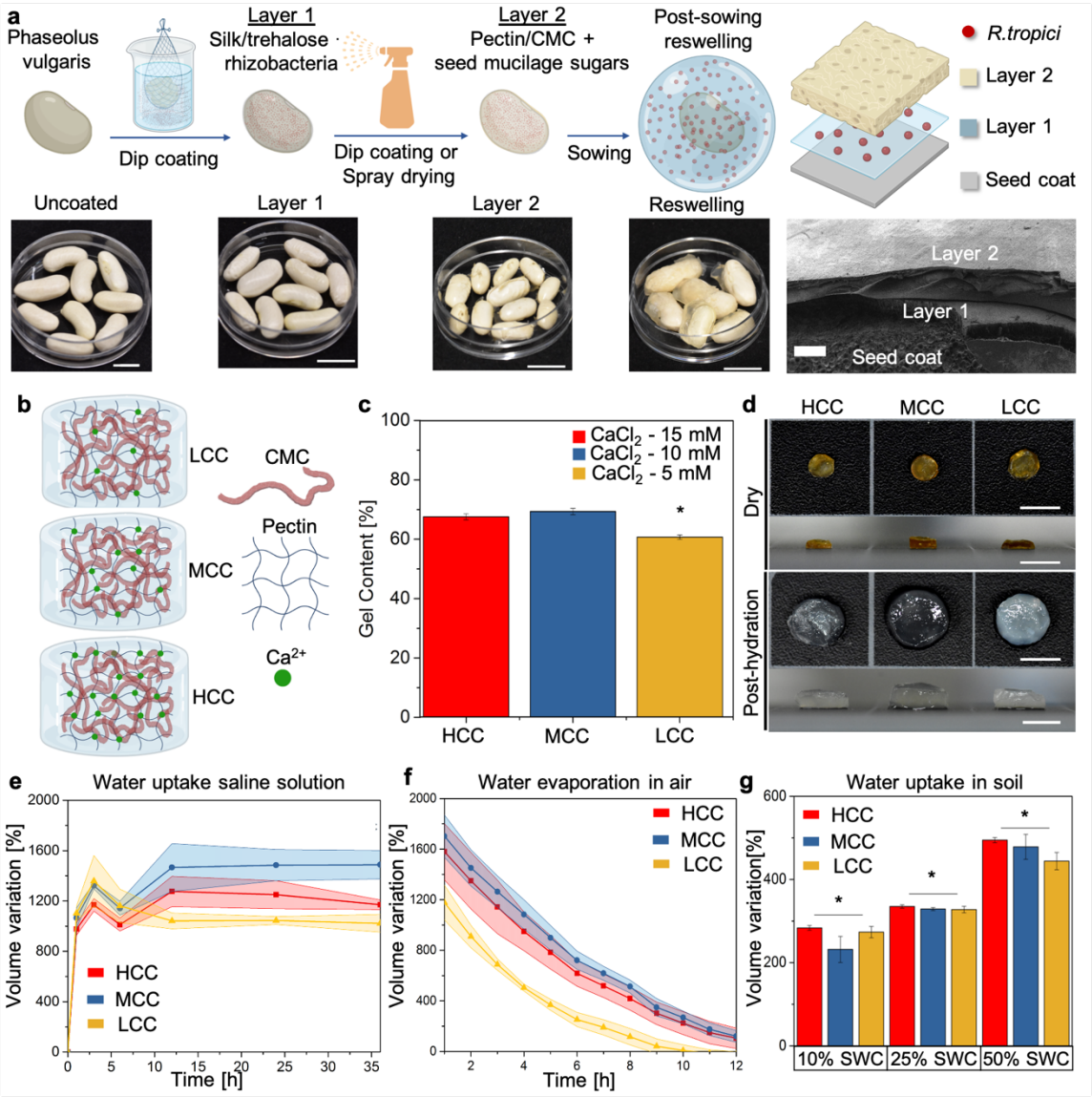

Fig. 1. Material design, fabrication and selection. a) Schematic diagram of the two-layered seed coating fabrication process, relative pictures of *P. vulgaris* coated seeds and crossection of coated seeds. Layer 1 contains a 1:3 mixture of silk-trehalose that adheres on the silk coat, encapsulates, preserves and releases *R. tropici* CIAT 899. Layer 2 is made of a 1:1 mixture of pectin-CMC (P:C). When the seed is watered, Layer 2 swells into a hydrogel and hydrates Layer 1, which dissolves and releases *R. tropici* CIAT 899. The hydrogel provides an appropriate environment for *R. tropici* CIAT 899 resuscitation and growth. Scale bars fo pictures correspond to 10 mm. Scale bar for SEM image of the coating is 10 µm b) Schematic of the pectin-CMC hydrogel structure, where Ca^{2+} are used to crosslink pectin chains while CMC acts as a filler to enhance water uptake. c) Effects of high, medium and low Ca^{2+}concentrations (HCC, MCC and LCC) on gel content. Stars above bars indicate a statistically significant difference in the mean of a material ratio group compared to all other groups (* $p<0.05$). The black error bars represent the standard error of the mean. d) Representative images of dry and swollen (12h in 154 mm NaCl solution) hydrogels. Scale bars=10 mm. e) Water uptake over time of dried P:C in 154 mm NaCl solution. f) Water evaporation over time of hydrogels after a 12h immersion in 154 mm NaCl solution. Highlighted areas around curves correspond to the standard error of the mean. g) Water uptake of P:C hydrogels in soils of increasing moisture content after 24h. Stars above bars indicate a statistically significant difference in the mean

swelling ratio of a soil humidity group compared to all other groups (* $p<0.05$). No statistical significant difference was found in the mean swelling ratios between $CaCl_2$ concentrations at similar soil humidity. The black error bars represent the standard error of the mean.

Fig. 2

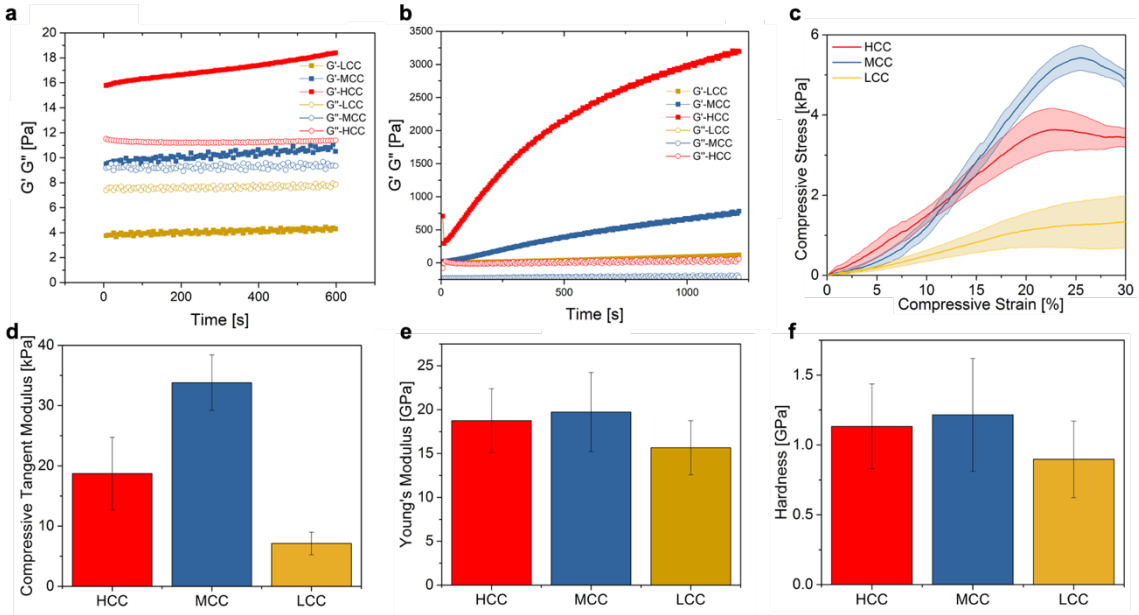

Fig. 2. Mechanical characterization of P:C hydrogels. a) Storage (G') and loss modulus (G") prior to NaOH addition. b) Storage (B') and loss modulus (G") after NaOH addition (last step in hydrogel fabrication process). c) Unconfined compression of P:C post hydration for 12h in 154 mm NaCl solution. Highlights around the curves correspond to the standard error of the mean. d) Calculated compressive tangent Young's moduli post hydration for 12h in 154 mm NaCl solution. Statistical significant difference in the mean Young's moduli of MCC compared with LCC (* $p<0.05$). e) Young's moduli on dry P:C hydrogels measured from nanoindentation studies. No significant statistical difference was measured in the young's moduli of dried materials. f) Hardness of dry P:C 1:1 measured with nanoindentation. No significant statistical difference was measured in the hardness of dried materials. The black error bars represent the standard error of the mean.

Fig. 3

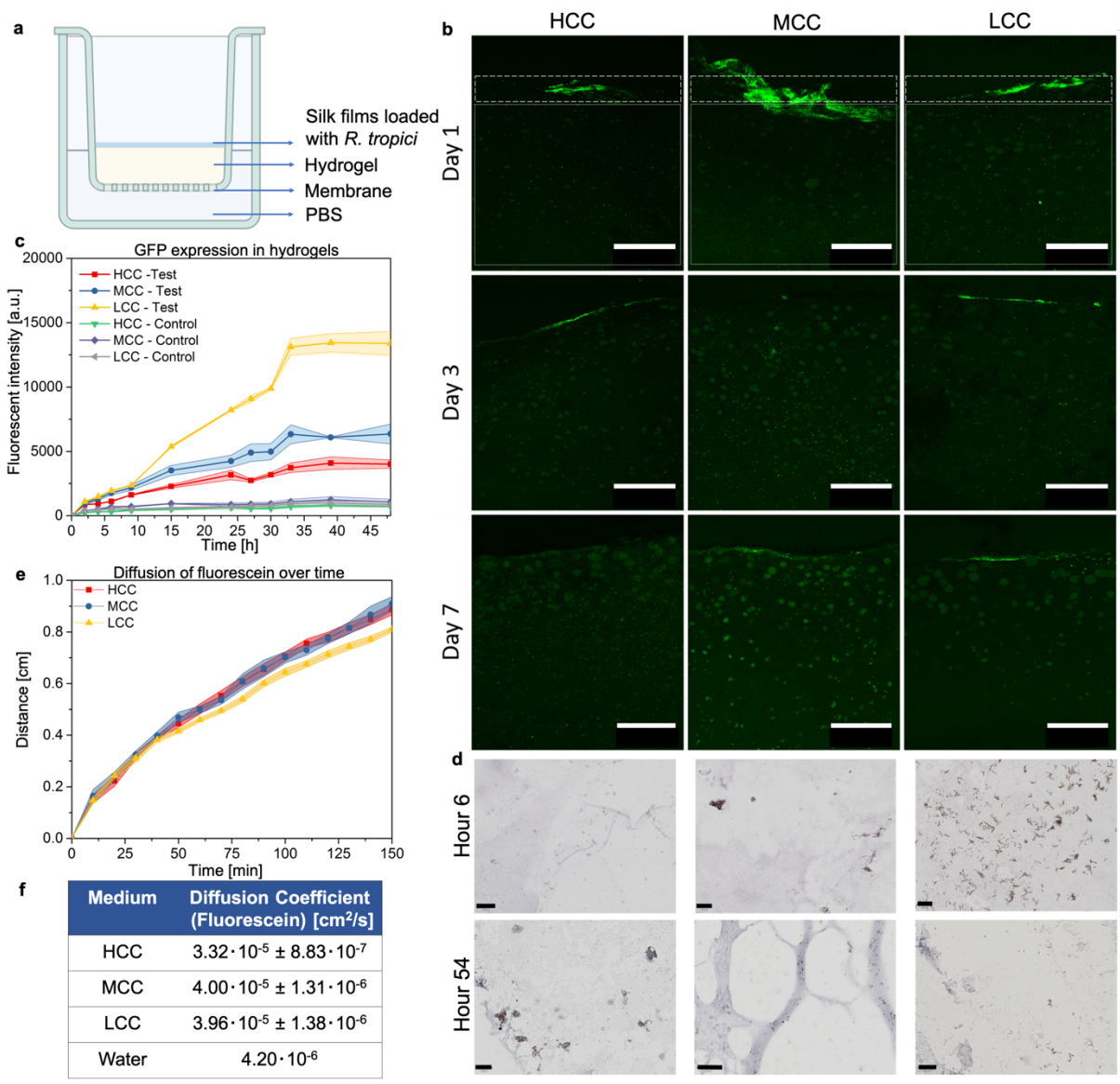

Medium	Diffusion Coefficient (Fluorescein) [cm²/s]
HCC	$3.32 \cdot 10^{-5} \pm 8.83 \cdot 10^{-7}$
MCC	$4.00 \cdot 10^{-5} \pm 1.31 \cdot 10^{-6}$
LCC	$3.96 \cdot 10^{-5} \pm 1.38 \cdot 10^{-6}$
Water	$4.20 \cdot 10^{-6}$

Fig. 3. Use of P:C hydrogels as niche to grow *R. tropici* post rehydration. a) Experimental setup showing *R. tropici* CIAT 899 released from silk films, migrating and growing in P:C hydrogels simulating dry to swollen states. b) Representative confocal cross-sections images showing microbe migration and growth in hydrogels, simulating post-sowing phenomena in soil. Dotted box highlights applied silk film location. Setup of experiment is shown in (A). Scale bars represent 500 μm. c) *R. tropici* CIAT 899-GFP expression in hydrated hydrogels, using the polysaccharides as only energy source. Highlighted areas around curves correspond to the standard error of the mean. d) Representative histology sections of the hydrogels used as only energy source, showing attraction of microbes in the hydrogels. Scale bars represent 20 μm. e) Diffusion of fluorescein in hydrogels to model movement of nutrients/sugars. f) Calculated diffusion coefficients.

Fig. 4

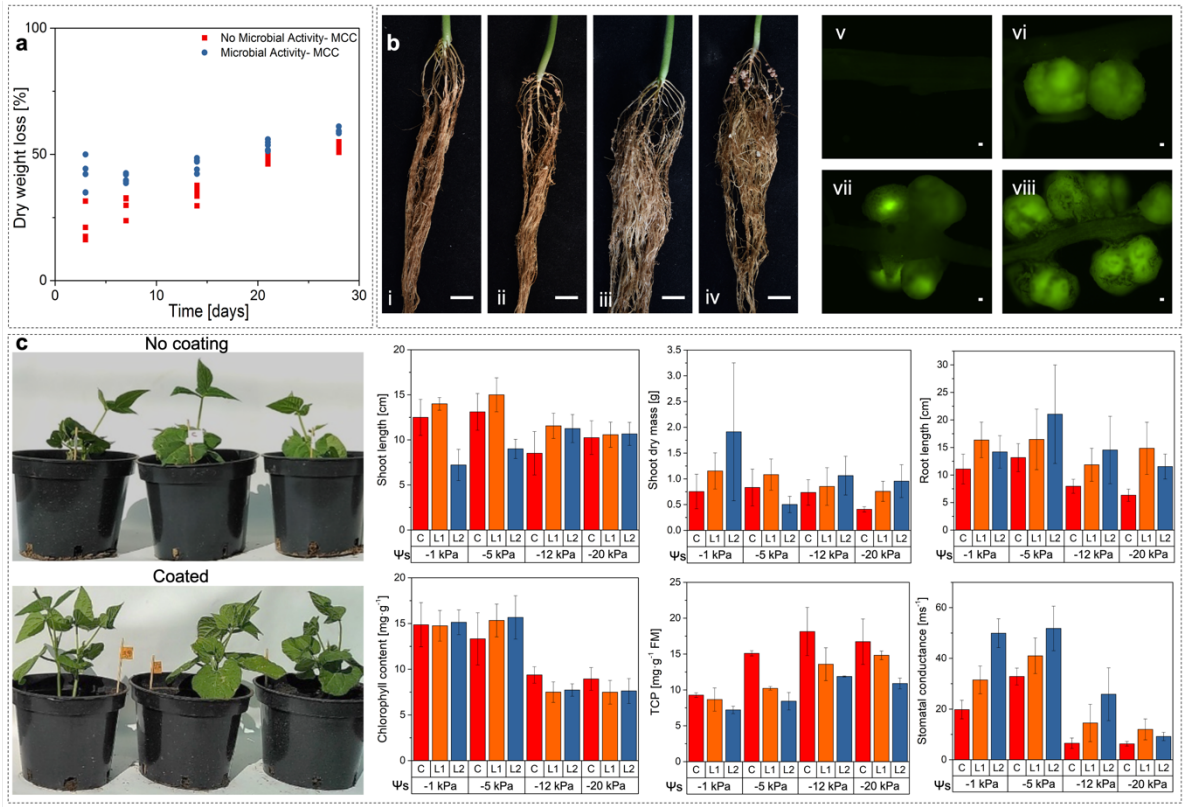

Fig. 4. Degradation in soil of seed coating material and application to *P. vulgaris* to mitigate water stress. a) Degradation of P:C hydrogel with soil microbe activity and without soil microbe activity in 25% humidity soil over a month at 16ºC. Dots correspond to collected data. b) Representative root images and corresponding fluorescent microscopy images of nodule formation for plants established from the following treatments: *i*) and *iv*) no coating and no inoculation; *ii*) and *vi*) inoculation of *R. tropici* CIAT 899-GFP using a 3% PVP solution; *iii*) and *vii*) bilayer coating with Layer 2 applied via spray-coating; and *iv*) and *viii*) bilayer coating with Layer 2 applied via dip-coating. Scale bars represent 10 mm for roots pictures and 100 μm for fluorescent microscope images. N=18 plants were tested per treatment type with a 100% nodulation rate for seeds treated with *R. tropici* CIAT 899. No nodulation was visible at day 14 for the negative control. c) Growth of *P. vulgaris* at week 6 in water stress regime for seeds that had no coating and that were coated with L1 and L2 coatings. *P. vulgaris* establishment investigation is shown as a function of coating and water potential (Ψs) levels. Ψs = -1kPa and -5 kPa correspond to healthy soil moisture content. Ψs = -12kPa and -20 kPa represent mild and severe water stress conditions, respectively. *P. vulgaris* plant establishment has been investigating by measuring shoot length, shoot dry mass, root length, chlorophyll content, total phenolic content (TPC) and stomatal conductance. Error bars represent standard deviation; five repeats were used per analysis and condition.